Andromeda: A mission to determine the gamma-ray burst distance scale

F.A. Harrison, W.R. Cook, T.A. Prince, S.M. Schindler
Space Radiation Laboratory, California Institute of Technology
Pasadena, CA 91125

C.J. Hailey
Columbia Astrophysics Laboratory
Columbia University, N.Y.C., NY 10027

S.E. Thorsett
Joseph Henry Laboratories and Department of Physics
Princeton University, Princeton NJ 08544

ABSTRACT

Andromeda is a wide-field, imaging, hard X-ray/soft gamma-ray instrument capable of detecting gamma-ray bursts (GRBs) a factor ~20 times fainter than *GRO*/BATSE. During 1-year of a two-year mission, it could determine whether GRBs are Galactic or cosmological in origin by searching for an excess of bursts towards the nearby Andromeda galaxy (M31). As a pointed, imaging instrument with sensitivity in the 10—200 keV band significantly better than previous coded-aperture instruments, *Andromeda* is capable of carrying out important secondary science objectives: for example, studying the soft-gamma-repeater and X-ray transient populations of M31 and the Galactic bulge. *Andromeda* is a coded aperture gamma-ray telescope consisting of a hexagonal coded mask coupled to an alkali-halide imaging scintillation detector, a flight-proven technology adapted from the balloon-borne Caltech Gamma-Ray Imaging Payload (GRIP). The new instrument is optimized for the 10–200 keV band and has 1.5° angular resolution over a 17° FWHM field of view. *Andromeda* is designed to be a small, low-cost mission, and draws its design largely from existing instrumentation. *Andromeda* was submitted to the STEDI program, and will also be proposed as a NASA Small Explorer.

Keywords: bursts, gamma-rays, small missions

1 SCIENTIFIC OBJECTIVES

1.1 · Gamma-ray Bursts

Gamma-ray bursts (GRBs) were discovered by the first small gamma-ray satellites placed in orbit, nearly thirty years ago.[4] Despite enormous advances in observational sophistication since then, the origin of these mysterious high-energy events remains unknown. The Burst and Transient Source Experiment (BATSE) on the *Compton Gamma-Ray Observatory* has made significant progress by a strategy of high-sensitivity burst observations with nearly uniform sky coverage. The isotropy of its large sample of GRBs together with the confirmation that there are fewer faint bursts than expected for an isotropic distribution rule out the hypothesis that bursts arise on the surfaces of nearby (disk popu-

0-8194-1877-3/95/$6.00

lation) neutron stars. Instead, two classes of models, both consistent with the BATSE observations, are widely discussed: those that place the bursts in a wide ($\gtrsim$ 100 kpc) Galactic 'corona,' with a scale size large compared to the Earth's galactocentric radius, and those that place the bursts at cosmological distances (z$\sim$1).

Burst sources in an extended Galactic corona may either be neutron stars born with high-velocity (600–800 $\mathrm{km\,s^{-1}}$) in the disk[7,8] or an old population born in the halo.[1] At distances of $\sim$100 kpc, luminosities of $10^{40} - 10^{41}$ $\mathrm{erg\,s^{-1}}$ are required, well above the Eddington luminosity of a neutron star. This need not be a problem: soft gamma repeaters, believed to be associated with neutron stars,[5] reach luminosities over 10^{41} $\mathrm{erg\,s^{-1}}$, and the 5 March 1979 burst from SGR 0526−66 had a spectrum similar to a classical GRB.[9] Cosmological distributions are attractive as they naturally account for the isotropy of the burst sources, the paucity of weak bursts being due to geometric limitations or source evolution. The required luminosity of 10^{51}–10^{52} $\mathrm{erg\,s^{-1}}$ could be produced through the gravitational-radiation-driven merger of two neutron stars in a binary system, for example. As with Galactic models, the origin of the burst spectrum and temporal variability is poorly understood.

Coronal halo models of GRBs predict similar burst halos around other massive spiral galaxies. *Andromeda* is designed with sufficient sensitivity and coverage to detect such a corona if it exists around M31, our nearest-neighbour spiral galaxy. In order to achieve its objective, *Andromeda* must both detect fainter bursts than BATSE and have a large enough field of view to sample bursts from a significant fraction of M31's burst corona. However, instrumental background effects make sensitivity and field of view competing goals. *Andromeda* is designed to achieve excellent sensitivity over a 17° FWHM field of view, which represents the optimum tradeoff for the coronal models allowed by BATSE's measurements.

Typical coronal models place the faintest bursts seen by BATSE at $\sim$ 300 kpc, though they may be as near as 150 kpc.[2] M31 is at a distance of $\sim$ 670 kpc, which then sets the sensitivity requirement for *Andromeda*: to rule out all halo models, it must be capable of detecting some bursts which are $(670/150)^2 = 20$ times fainter than BATSE's faintest bursts. Of course, this is the most conservative case, and some bursts will be detected first from the near side of M31's halo, but the number depends on extrapolation of the halo distribution in M31 beyond the radius observed in our Galaxy by BATSE.

Andromeda's substantial sensitivity improvement over BATSE derives from three advantages: (1) a reduced detector background due to collimation and shielding, (2) an energy band optimized for burst detection, and (3) trigger integration times optimized for burst detection. The ratio of the distance at which *Andromeda* can detect a burst to the distance at which BATSE can detect a burst will thus depend on the burst spectrum and duration. A more detailed description of the instrument sensitivity is given in Section 4. For illustration, approximately 25% of BATSE's burst sample would be detectable by *Andromeda* if they were 20 times fainter than the BATSE detection threshold.

The range of acceptable halo sizes (150 – 400 kpc) implies that M31's corona will subtend 20° – 60° on the sky, and thus a large FOV must be observed to detect a possible M31 corona (one kiloparsec at M31 subtends 5 arcmin). If the instrument FOV does not cover the entire burst corona, the detection rate will depend on the burst radial distribution. A Galactic GRB distribution is often parameterized with a form appropriate for the dark matter halo:

$$\rho(r) \propto \frac{1}{1 + (r/r_c)^{\alpha}}, \tag{1}$$

Table 1: Number of excess bursts detectable towards M31 relative to a control field by *Andromeda* per year for various values of the BATSE sampling distance. Minimum and maximum rates are extremes obtained by varying model parameters in Equation 1 subject to consistency with the BATSE moment constraints.

$R_{\rm samp}$ (kpc)	# excess bursts/year	
	minimum	maximum
150	71	74
250	235	338
350	150	252
control field	total bursts/year (max) : 22	

where r_c is the core radius and $\alpha = 2$ for an asymptotically flat rotation curve. Assuming this distribution and that all bursts have the same peak flux (the "standard candle" assumption), the angular moment and luminosity constraints imply that BATSE is observing bursts to a distance between 150 and 400 kpc.[2] This parametrization is somewhat arbitrary, other radial distributions being possible. However, for a large FOV instrument such as *Andromeda*, the burst detection rate is relatively insensitive to the exact form chosen for the radial distribution, but depends primarily on the characteristic size of the halo, and the distance to which BATSE is observing its weakest bursts (which are directly constrained by the BATSE moment distribution).

We have calculated the number of detectable bursts expected for those coronal models consistent with the BATSE data set, assuming a burst spatial density distribution given by Equation 1 and standard candle luminosities. Table 1 gives the expected detection rate for a range of $R_{\rm samp}$, where the minimum and maximum values for a given $R_{\rm samp}$ indicate the minimum and maximum rates for the range of model parameters consistent with the BATSE data. Details on the method used to determine the detection rates can be found in [Harrison and Thorsett, 1995].[3] Also indicated in Table 1 is the number of bursts expected in a control field, calculated by extrapolating the BATSE number - flux relationship to the instrument threshold. This should yield an upper-limit to the background burst rate, above which a burst excess is to be detected. We have demonstrated through simulations that the standard candle assumption represents a worst-case for detection, as addition of a luminosity function results in a larger fraction of bursts falling above the detection threshold.

If *Andromeda* fails to detect an excess of bursts in the direction of M31, extended Galactic distributions will be ruled out, leaving cosmological distributions as the last viable alternative. In this event, *Andromeda's* sensitive burst searches can be used to constrain the form of the burst number-luminosity relationship well-below the BATSE threshold, thus limiting source evolution, luminosity function, and redshift distribution for a given cosmology.

1.2 Other science objectives

In addition to its primary capabilities for studying gamma-ray bursts, *Andromeda* will be a sensitive instrument for imaging observations of other hard X-ray and soft gamma-ray sources. Figure 1 com-

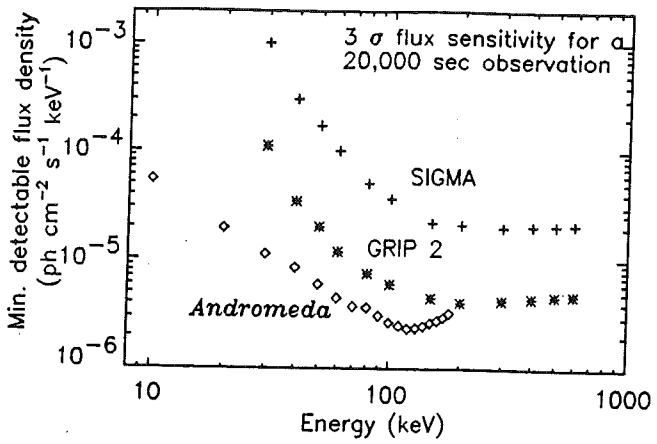

Figure 1: A comparison of the instrument sensitivity of *Andromeda* to that of *Granat*/SIGMA and the Caltech GRIP-2 balloon experiment. The sensitivity is calculated for a 3σ detection in a 20,000 s observation, assuming an energy bandwidth $\Delta E/E$ of 0.5. Note that *Andromeda* is optimized to provide high-sensitivity at energies < 200 keV.

pares the flux sensitivity of *Andromeda* and SIGMA, an instrument recently flown on the Russian/French *GRANAT* mission. SIGMA was a pioneering imaging mission for hard X-ray/soft gamma-ray observations and achieved its success despite a small effective area, making important new observations of transient X-ray novae, candidate black hole systems, and low-mass X-ray binary sources in the Galactic bulge. *Andromeda* (10–200 keV) is at least an order of magnitude more sensitive than SIGMA and will be able to continue and extend SIGMA's successful program of imaging observations. This is especially important to complement observations by *GRO*, whose instruments have at best $\sim 3°$ source positioning capability in *Andromeda*'s energy range.

2 MISSION DESCRIPTION

The desired mission lifetime for *Andromeda* is two years. Six months of the first year of operation would be devoted to observations of M31 (required to address the range of possible halo models). Pointings sufficiently removed from M31 would serve as control observations to measure the background burst rate, but would also contain other targets of astrophysical interest. In order to simplify mission planning and minimize ground-support costs, the remaining time would be devoted to long, dedicated observations and selected target of opportunity pointings. For example, long observations of the Galactic center region to monitor the hard X-ray transient population, and surveys of selected regions of the plane are attractive possibilities.

The baseline mission assumes a circular 28°inclination low-earth orbit. The spacecraft utilizes fixed, body-mounted solar panels, and thus the pointing plan is constrained by the need to keep the solar angle to the pointing axis in the range $45° < \theta_{\rm Sun} < 135°$. Given this constraint, both M31 and the Galactic center are observable for nine months of the year, with little overlap between restricted viewing

Table 2: Instrument characteristics and telescope configuration

Instrument Characteristics	
Energy Range	10 – 200 keV
Angular Resolution	1.5°
Field-of-View	17°FWHM
Strong Source Positioning	0.1°
Orbit	Low Earth Orbit (nominal 28°inclination)
Telescope Configuration	
Detector	NaI - 3 mm / CsI - 2 cm phoswich
Geometric Area	2200 cm^2
Energy Resolution	12% @ 122 keV
Collimator	Lead Hexcell
Mask	Hexagonal URA Coded Aperture - 3 mm Lead
Mask Pixel Size	2.6 cm
Mask-Detector Spacing	1 m

periods. The duty-cycle for observations would be ~60% due to earth occultation and SAA passage, as no reorientation during earth blockage would be planned.

3 INSTRUMENTATION

Andromeda is a sensitive coded-aperture telescope optimized for the detection of gamma-ray bursts. A hard X-ray photon entering the instrument through a coded-aperture mask (which consists of a pattern of opaque and transparent elements) is absorbed by an alkali-halide detection element (see Figure 2). The resulting scintillation light is detected by photomultiplier tubes (PMTs) coupled to the back of the crystal assembly and is converted into electronic pulses. The signal in each PMT is read out and digitized, and the ratio of the signal amplitudes is used to determine the interaction position of the X-ray. The summed signal is proportional to the total energy deposited in the crystal. The coded aperture spatially modulates the incoming X-ray flux, so source positions can be reconstructed by postprocessing of the spatial distribution of detector counts. Pulseheight, position and time will be individually stored and telemetered to the ground, providing capability for fast timing and image reconstruction on the ground. The key instrument parameters are summarized in Table 3. Many aspects of the *Andromeda* are based directly on the Caltech *GRIP-2* balloon instrument,[10] including the large-area phoswich detector, coded mask imaging system, and event readout and processing. An overview of the major aspects of the instrumentation is presented in the following sections.

3.1 Phoswich detector

The *Andromeda* detector consists of a 53.3 cm diameter, 3 mm thick NaI(Tl) scintillator crystal optically coupled to a hexagonally-segmented 2 cm thick CsI(Na) Compton rejection shield and read

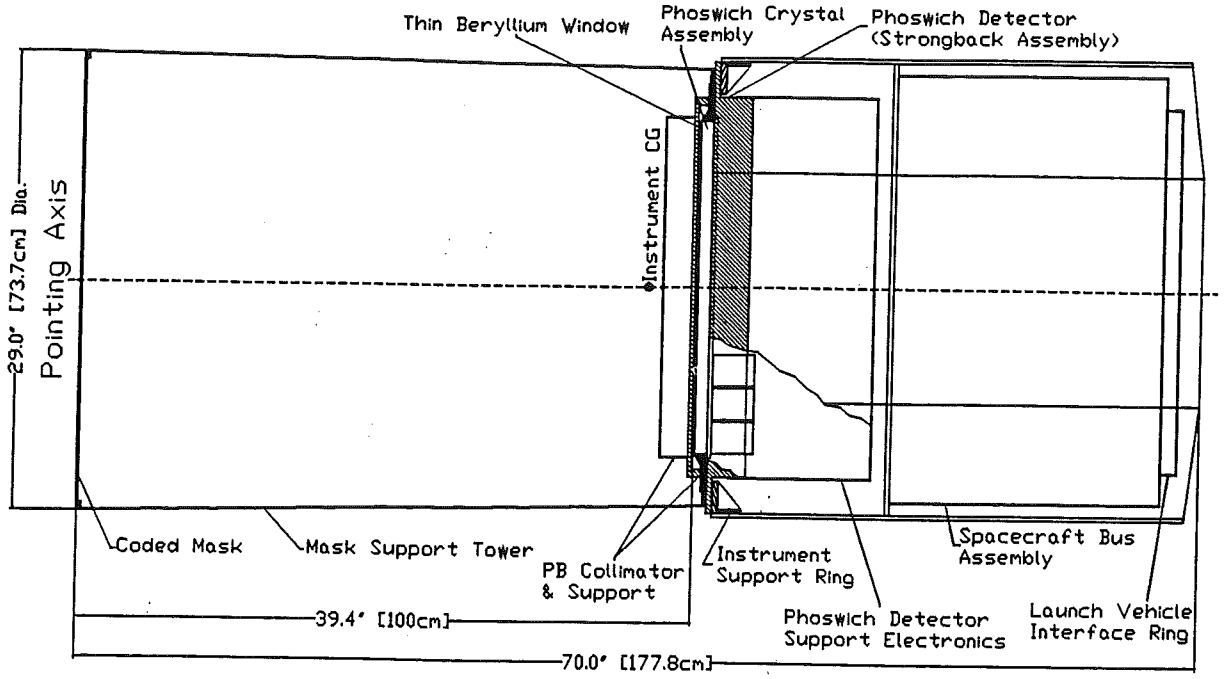

Figure 2: Diagram of the instrument and bus

out by 61 PMTs. It is directly scaled from the GRIP-2 imaging phoswich, but with a thinner NaI detection element (optimized for lower energies) and smaller active area (2200 cm^2 compared to GRIP's 3800 cm^2). For phototube readout we have selected a ruggedized version of the Hamamatsu R1840 PMT. A thin beryllium entrance window provides high transparency to X-rays in the range of interest. Performance parameters have been directly scaled from GRIP-2.

3.2 Electronics and data processing

An overview of *Andromeda*'s detector readout electronics is shown in Figure 3. The 61 PMTs viewing the NaI/CsI phoswich camera plate will each be instrumented with an analog readout chain consisting of a preamplifier, shaping amplifier, low, middle, and high level discriminators, dual gated integrators, and dual 8-bit Wilkinson-type analog-to-digital converters. Event processing will start whenever any of the lower level discriminators associated with the individual PMTs trigger. After such a trigger, the gated integrators will be operated in unison so that, for each tube, two 8-bit results are obtained: one for a 0.5 μs integration period and the second for a 1.0 μs period. The middle and upper level discriminators will define a window containing the X-ray events of interest. Events outside the window, including charged particle events (at high energies) and very low energy X-rays, will be immediately rejected.

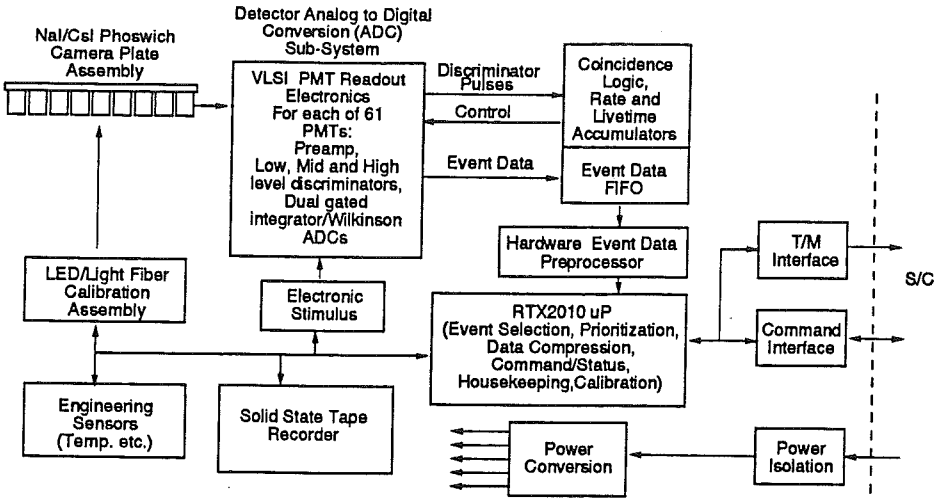

Figure 3: Block diagram of the *Andromeda* electronics.

The Wilkinson rundown counter will clock at 64 MHz, allowing the maximum 256 count conversion to be accomplished in only 4 μs. This high speed and low dead time per event allows pulse-height analysis of all X-ray events, and eliminates the need for sophisticated circuitry to reject CsI shield events in real-time. Instead, CsI event background rejection, as well as X-ray event energy and position determination, will be done using analysis of the dual integration period pulse height data by the high-speed on-board microprocessor.

The analog readout chains will be implemented entirely in radiation-hardened, custom CMOS VLSI circuitry. The advantages of the VLSI approach include low power, low weight, and reduced cost and schedule risks through a large reduction of parts count. All 61 PMTs will be read out with only 8 VLSI chips, each containing the complete analog front-end electronics for 8 tubes and operating on only 30 mW per tube. The use of an existing, low-noise preamplifier design will allow the PMTs to be run at relatively low gain and high reliability.

3.3 Spacecraft

Table 3 summarizes the mission requirements for the spacecraft. The modest pointing, power and aspect reconstruction accuracy required by *Andromeda* allow the use of off-the-shelf small satellite bus technology. We have specified a baseline system which is almost a direct copy of the AeroAstro *HETE* spacecraft bus. This system is capable, low-cost, and will be flight-proven in the near future. The spacecraft is spin-stabilized (rotation about the telescope long-axis), and provides power through fixed, body-mounted solar panels. Further stabilization and the capability to re-orient are provided by magnetic torque coils. The spacecraft attitude is determined by magnetometers, sun sensors, and a horizon-crossing indicator.

Table 3: Spacecraft requirements and AeroAstro specifications

Parameter	Design requirement	AeroAstro specification
Pointing and Aspect		
Max. deviation of ptg axis from target (3σ)	$\pm 3°$	$\pm 2°$
Stability (max. drift rate)	$< 3°$/hr	1°/hr
Aspect knowledge (3σ)	0.2°	0.1°
Aspect reorientation time	~1 day	few hrs
Reorientations	2-6 whole mission	unconstrained
Solar angle	Exclude Sun from FOV	$45° < \theta_{\rm Sun} < 135°$
Spin rate (about pointing axis)	0–5 rpm	2 rpm
Average Power		
Instrument	10 W	
Spacecraft	21 W	
Total	31	40
Telemetry		
Data rate	30 kbps (orbit avg)	
Max. downlink bit error rate	10^{-5}	10^{-5}

4 SENSITIVITY

4.1 Continuum sensitivity

The background-limited flux sensitivity of a coded-aperture telescope is given by:

$$F_K = \frac{2K}{\eta \epsilon t_i t_c (1 - t_m)} \left[\frac{B}{A \tau \Delta E} \right]^{1/2}, \tag{2}$$

where F_K is source flux (in photons cm^{-2} s^{-1} keV^{-1}) which can be detected with statistical significance K; η is the imaging efficiency, an order-unity factor which accounts for the loss of sensitivity due to finite detector position resolution relative to coded-aperture cell-size; ϵ is the full-energy photon detection efficiency; t_i is the fraction of source photons transmitted through passive material in the instrument (i.e., a Be detector entrance window and Carbon fibre mask support); t_c is the fraction of source photons transmitted through the Pb collimator, taken as 0.95 for normal incidence; t_m is the fraction of source photons transmitted through closed coded-aperture cells; B is the detector background counting rate in photons cm^{-2} s^{-1} keV^{-1}; A is the usable geometrical area of the detector; τ is the observation livetime in seconds; ΔE is the width of the energy interval for the flux measurement, in units of keV.

The above expression is identical to that for the sensitivity of an ideal "source on - source off" measurement, with the exception of the factors η and $(1 - t_m)$, which have values near unity. Most of the parameters on which the sensitivity depends may be calculated with negligible error. The one exception is the detector background, which is discussed in the following section. The sensitivity calculation for *Andromeda* is illustrated in Table 4. The observation time, τ, has been taken as 2×10^4 seconds, the detector area, A, as 2200 cm^2, the detection significance is 3, and the energy bandwidth, $\Delta E/E$, as 50%.

Table 4: Continuum sensitivity for *Andromeda*

E (keV)	B (ph cm^{-2} s^{-1} keV^{-1})	ϵ	η	t_i	$F_{3\sigma}$ (ph cm^{-2}s^{-1} keV^{-1})
10	83×10^{-4}	0.80	0.85	0.79	60×10^{-6}
20	35×10^{-4}	0.99	0.92	0.92	21×10^{-6}
30	17×10^{-4}	0.99	0.95	0.97	12×10^{-6}
50	6.0×10^{-4}	0.85	0.97	0.98	6.0×10^{-6}
100	2.0×10^{-4}	0.76	0.99	0.99	2.7×10^{-6}
200	0.73×10^{-4}	0.27	0.99	0.99	3.3×10^{-6}

As an illustration of the above sensitivity calculation, the detection limit for $K = 5.5\sigma$ for a ten second integration over the energy band 10 - 200 keV for a source with a photon spectral index $\gamma = 2$ is $1.6 \times 10^{-9}\,\mathrm{erg\,cm^{-2}\,s^{-1}}$.

4.2 Detector Background

The average background has been estimated for a low-Earth orbit with 28° inclination. For this orbit the background count rate is variable. Several components of the internal detector background vary with the rigidity cutoff of the primary cosmic ray spectrum (which varies as a function of latitude). The activation history of the detector is also important and this varies during a single orbit and also over several orbits (primarily due to the time since last SAA passage).

Our detector background calculations are scaled from background measurements made during the GRIP-2 flight from Palestine, TX (rigidity cutoff = 4.7 GV). The shield leakage and Compton scattered components are determined by subtracting the aperture contribution from GRIP's background and scaling by the crystal volume. This represents an upper limit, since the angle subtended by the atmosphere decreases with altitude, and is smaller for a satellite than for a balloon. The contribution from neutrons and spallation were derived by scaling from previous spaceborne scintillation detectors, accounting for the charged particle environment specific to our orbit. The expected background count rate as a function of energy is shown in Figure 4. Below about 40 keV, the background is dominated by diffuse aperture flux, with internal detector background becoming important at higher energies. The internal background component is uncertain to a factor of ~two.

4.3 Burst sensitivity

Because of the diversity of GRB spectra and timescales, there is no unique measure of the sensitivity of *Andromeda* relative to BATSE. Rather, the question is: for a large number of bursts detected by BATSE, what is the significance with which *Andromeda* would detect these same bursts? Given Equation 2, we can calculate the significance with which *Andromeda* will detect a burst of a given spectrum and duration. For the same burst, we can calculate the detection significance for BATSE from knowledge of the BATSE detector response and background count rate. We have simulated detections for a sample of bursts with various time and energy profiles for both BATSE and *Andromeda*. For BATSE,

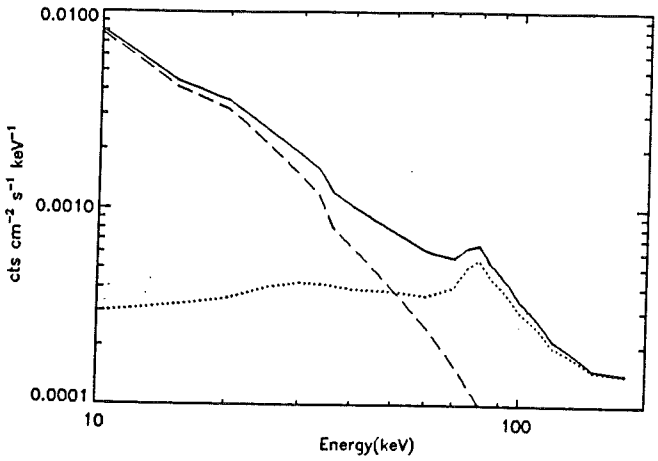

Figure 4: Total average instrumental background count rate.

we assume the most favorable case, corresponding to a burst located at an off-axis position equidistant between two detectors. (BATSE requires detection above threshold in more than one detector to trigger on a burst.) We used the instrument response matrices distributed by the BATSE team (which account for the angular and energy-dependent detector response) and typical measured background count spectra. Time profiles were taken from 420 bursts detected by the BATSE LADs and energy profiles from 54 bursts having well-characterized spectra were used. A plot of the relative detection sensitivities of *Andromeda* and BATSE for this simulated sample of bursts is shown in Figure 5.

This method of estimating the sensitivity is conservative for several reasons. First, the sample of bursts used is biased towards those with hard emission. The average X-ray (2–10 keV) to gamma-ray (2–375 keV) flux ratio of the sample is lower than that of bursts detected by *Ginga*[11] and XMON,[6] both of which triggered at a lower energy than BATSE. Second, the sample is probably also biased toward short-duration bursts given that the longest BATSE trigger timescale is 1 s. The underlying burst distribution is likely to include softer, longer bursts which were missed by BATSE, increasing the number detectable by *Andromeda.*

5 CONCLUSION

The clearest distinction between galactic and extragalactic source models is the prediction of galactic models that burst halos should exist around neighbors of the Milky Way. In order to optimize detection rates for burst coronae surrounding our nearest neighbor massive spiral galaxy, M31, an instrument with an order of magnitude better sensitivity over a FOV of $\sim 20^\circ$ is required. *Andromeda* is a simple, low-cost mission with these characteristics. In an observation time of 6 months, *Andromeda* can address the allowed range of Galactic coronal models. In addition, *Andromeda's* large FOV and imaging capability in the hard X-ray/soft gamma-ray band make it ideally-suited to carry out monitoring observations of the hard x-ray binary population of our Galaxy.

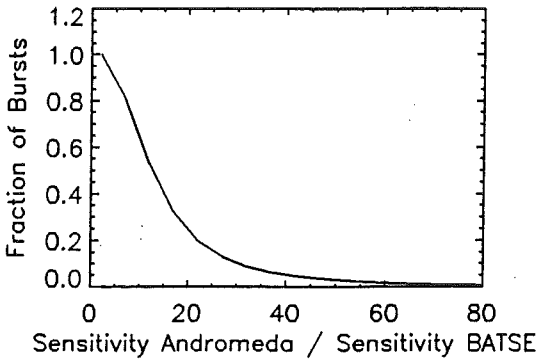

Figure 5: Relative burst detection sensitivity for *Andromeda* compared to BATSE, for the sample of bursts (drawn from the BATSE detections) used in our calculations.

6 REFERENCES

[1] J.J. Brainerd. *Nature*, 355:522, 1992.

[2] J. Hakkila, C. A. Meegan, G. N. Pendleton, G. J. Fishman, R. B. Wilson, W. S. Paciesas, M. N. Brock, and J. M. Horack. Constraints on galactic distributions of gamma-ray burst sources from batse observations. *ApJ*, 422:659, 1994.

[3] F.A. Harrison and S.E. Thorsett. *ApJ*, submitted, 1995.

[4] R. W. Klebesadel, I. B. Strong, and R. A. Olson. Observations of gamma ray bursts of cosmic origin. *ApJ*, 182:L85, 1973.

[5] S.R. Kulkarni and D.A. Frail. *Nature*, 365:33, 1993.

[6] J. G. Laros, W. D. Evans, E. E. Fenimore, R. W. Klebesadel, S. Shulman, and G. Fritz. 3–10 kev and 0.1 to 2 mev observations of four gamma-ray bursts. In S. E. Woosley, editor, *High Energy Transients in Astrophysics*, page 378, New York, 1984. AIP Press.

[7] H. Li and C.D. Dermer. *Nature*, 359:132, 1992.

[8] P. Podsiadlowski, M.J. Rees, and M. Ruderman. *MNRAS*, 273:755, 1995.

[9] P. V. Ramana Murthy and A. W. Wolfendale. *Gamma-Ray Astronomy.* Cambridge U. Press, Cambridge, 2nd edition, 1993.

[10] S.M. Schindler et al. *NIM*, to be submitted, 1995.

[11] A. Yoshida, T. Murakami, M. Itoh, J. Nishimura, T. Tsuchiya, E. E. Fenimore, R. W. Klebesadel, W. D. Evans, I. Kondo, and N. Kawai. Soft x-ray emission from gamma-ray bursts observed with ginga. *Proc. Astr. Soc. Jap.*, 41:509, 1989.

ACKNOWLEDGEMENTS

We thank all of the members of the Andromeda Working Group (B. Pacyński, D. Chakrabarty, W. Craig, T. T. Hamilton, D. W. Hogg, S. R. Kulkarni, W. H. G. Lewin, P. Podsiadlowski, P. S. Ray, G. Sprehn, H. Tannenbaum) for their contributions to this work. FAH acknowledges support from a Robert A. Millikan Fellowship.